Astron. Astrophys. 278, 644–653 (1993)

ASTRONOMY AND ASTROPHYSICS

The location of secular resonances close to the 2/1 commensurability

A. Morbidelli, H. Scholl, and Ch. Froeschlé

Observatoire de la Côte d'Azur, B.P. 229, F-06304 Nice Cedex 4, France

Received January 21, accepted June 9, 1993

Abstract. This paper is devoted to the problem of the location of secular resonances close to a mean motion commensurability in the main asteroid belt. This is quite a difficult problem because of the presence of several resonances in the same part of the phase space, which makes it a dynamical system with strongly coupled degrees of freedom. Therefore, we apply here the perturbation method of "successive elimination of harmonics" in order to find out in the regular regions the proper frequencies of the system and, consequently, locate the secular resonances. In particular, we concentrate on the location of the ν_6 resonance close to the 2/1 commensurability, since this is related to the existence of the upper bound of the distribution of the inclinations of the asteroids between 3.0 and 3.2 A.U.. We confirm that, as suspected, the ν_6 resonance is at a larger inclination than the main asteroid population. Our theoretical findings are confirmed by several numerical integrations, with initial conditions systematically chosen on a suitable grid.

Key words: celestial mechanics – solar system: general – minor planets

1. Introduction

The location of secular resonances in the asteroid belt has been deeply explored in recent times, since the pioneering work of Williams (1969). This is a relevant problem from the astronomical point of view; indeed, secular resonances play a fundamental role in structuring the distribution of the asteroids in the main belt. In particular, the ν_6 resonance (which is the 1/1 resonance between the precession rate of the perihelion of the asteroid and that of Saturn), bounds the distribution of the inclinations of the asteroids in most parts of the belt.

Nowadays, the location of secular resonances is well understood, except in those regions of the belt which are very close to a mean motion commensurability (i.e. a commensurability between the orbital motion of the asteroid and that of Jupiter). Indeed, mean motion commensurabilities affect strongly the secular motion; in particular they change the proper secular frequencies and consequently also the location of secular resonances and their dynamical effect. From the mathematical point of view, the presence of a mean motion commensurability increases the number of strongly coupled degrees of freedom of the problem, which therefore turns out to be much more complex.

The history of the different attempts for the computation of the location of secular resonances shows the recent improvements in theoretical celestial mechanics and explains the motivations of this work.

The common approach for the study of the secular dynamics is the averaging of the Hamiltonian of the problem with respect to the mean anomalies of the asteroid and of the planet(s). This is done via the Lie alghoritm and gives the secular Hamiltonian under the form of a non–convergent power series in the mass of the perturbing planet(s).

In 1981, Williams and Faulkner determined the location of secular resonances taking into account only the linear term in the masses of the planets. The authors themselves suspected that this was a crude approximation in the vicinity of a mean motion resonance, since the neglected higher order terms diverge in correspondence of mean motion commensurabilities, due to the so called *small denominators*. This idea was supported also by the fact that, comparing their results with the present distribution of the asteroids, one could see that close to the 2/1 mean motion commensurability (semi–major axis in between 3.0 and 3.2 A.U.) the inclination of the asteroids is not bounded by the ν_6 resonance, as it happens for $a < 3.0$ A.U.

Some years later, Milani & Knežević(1990) computed for the first time the quadratic term in the masses up to degree 2 in the eccentricities and inclinations e and i of asteroid and planets. They pointed out in this way that the effect of mean motion commensurabilities is to shift secular resonances; in particular the 2/1 commensurability (the strongest one) deviates the ν_6 secular resonance at larger inclinations, so that one can understand the existence of asteroids with inclination above the ν_6 limit computed by Williams and Faulkner for $a > 3.0$ A.U..

Later, Morbidelli & Henrard (1991), computing the quadratic term in the masses up to degree 4 in e and i, pointed out that the results are very sensitive to the limit power degree of e and i used in these kinds of computations. Therefore the problem was open again.

A further step has been done in Lemaitre & Morbidelli (1992). In that work the quadratic term in the masses was com-

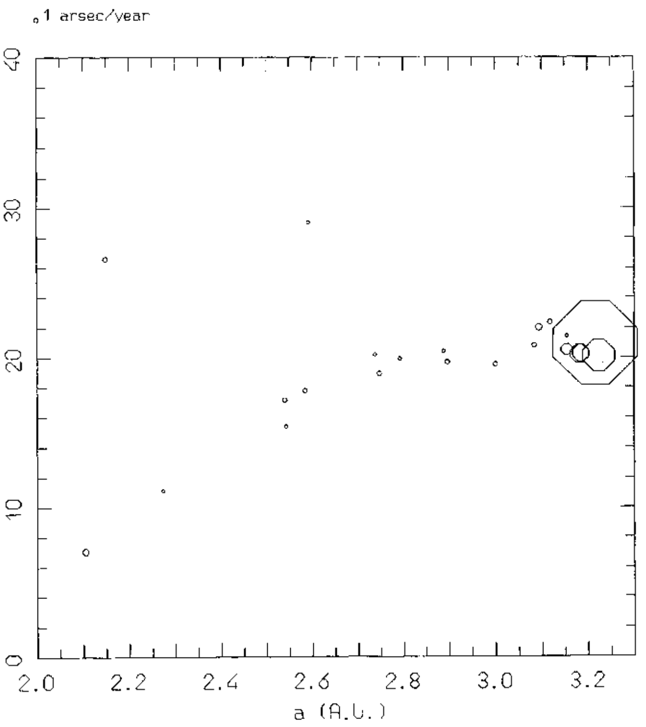

Fig. 1. The error in the computation of the proper frequency of the longitude of perihelion using the algorithm in Lemaitre and Morbidelli (1992). The size of each dot is proportional to the square root of the error in *arsec/year*

puted without any expansion in power series of the eccentricity and the inclination, thus avoiding the above mentioned problem. Nevertheless, some numerical tests show that the error in the computation of proper frequencies diverges approaching the 2/1 commensurability, as one sees in Fig. 1. This figure reports on the $(a - i)$ plane the error on the computation of the frequency of the longitude of perihelion, the size of each dot being proportional to the square root of the error in *arsec/year*. The explosion of the error can be explained by the fact that also the terms of order larger than 2 in the perturbation masses, which are still neglected, are actually important. As a matter of fact, the averaged Hamiltonian given by the Lie algorithm is a non–convergent series, which diverges abruptly close to a mean motion commensurability.

Therefore, in order to compute proper frequencies near a mean motion commensurability, one has to follow a different approach: instead of averaging the Hamiltonian of the problem over the mean anomalies of the asteroid and the planets (which produces the small denominator responsible for the divergence), one has to introduce first the critical angle σ of the mean motion commensurability, and afterwards average the Hamiltonian only over the non–resonant combinations of the mean anomalies. This allows one to avoid the small denominator associated with the mean motion commensurability, so that the terms of higher order in the masses are actually small and can be neglected. The price to pay is that the linear term in the masses, even in its most simplified form $\overline{K_0}$ (obtained by assuming the planets on coplanar circular orbits), depends now on two angles, namely the critical angle of the mean motion resonance σ and the argument of perihelion g. Consequently, the dynamics described by $\overline{K_0}$ is non–integrable.

A study of such dynamics has never been performed before, to our knowledge. The purpose here is to perform this study in order to determine the chaotic layers and the region of regular motion, and define in the latter suitable action–angle variables. These in turn provide the definition of "proper frequencies", which, compared to the proper frequencies of the planetary system, lead to determine the location of secular resonances. A similar approach has been recently followed by Morbidelli & Moons (1993), who have studied, by successive elimination of harmonics, the existence and the effects of secular resonances *inside* mean motion commensurabilities.

The mathematical tool we use in this paper is the perturbation method of *successive elimination of harmonics* introduced in Morbidelli (1993) and Morbidelli & Giorgilli (1993), which turns out to be particularly suitable for the study systems with two degrees of freedom, characterized by a strong interaction between the degrees of freedom.

As a matter of fact, the dynamical system we are dealing with is three-dimensional; however, the existence of one constant of motion independent of the energy allows to simplify partially the problem. Indeed, the phase space is foliated in surfaces corresponding to different values of this constant of motion, and, on each surface, the system is reduced to two degrees of freedom. A global picture of the dynamics is obtained by studying a suitable number of these surfaces. Three independent proper frequencies are computed: these are the frequencies of the argument of perihelion, of the longitude of perihelion and of the critical angle of the mean motion resonance. Luckily, the phase space turns out to be quite simple, so that only two steps of the algorithm for the eliminations of harmonics are required in practice.

In this way we compute here the location of secular resonances without passing through the computation of singular higher–order terms in the masses, thus obtaining, in principle, better results.

Our final result is illustrated in Figs. 6, 7 and 8 which confirm that the secular resonances are deviated by the presence of the 2/1 mean motion commensurability to a larger inclination with respect to the original computations by Williams and Faulkner. Therefore, the asteroids between 3.1 and 3.2 A.U. with inclination of about 20 degrees should not be affected by the ν_6 resonance.

This paper is structured as follows: in section 2 we illustrate the definition of the new model for the computation of proper frequencies, which depends on two angles. In section 3 we discuss the application of the successive elimination of perturbation harmonics to this model. In section 4 we discuss the final results and compare them with numerical simulations starting from initial conditions systematically chosen on a suitable grid, in order to determine experimentally the actual location of the ν_6 resonance.

2. A model for the location of secular resonances close to the 2/1 commensurability

We recall here the basic steps for the computation of the location of secular resonances that were followed by Williams (1969), Williams & Faulkner (1981), Morbidelli & Henrard (1991) and Lemaitre & Morbidelli (1992). First of all the Hamiltonian of the problem is expanded in series of powers of the eccentricities and inclinations of the planets. Furthermore, the Hamiltonian is averaged with respect to the mean longitudes of the asteroid and of the planets. The computation of the proper frequencies is based on the analysis of the most relevant term, which turns out to be the one obtained assuming the planets on coplanar circular orbits, usually denoted as $\overline{K}_0$. This term is integrable, since it depends only on one angle, i.e. the argument of perihelion g, as pointed out by Kozai (1962).

To be consistent with this scheme, we will take into account in the following only the perturbation caused by the planets on coplanar circular orbits (for simplicity we will consider only the perturbation caused by Jupiter). The difference with respect to the above quoted works is that, assuming now to be close to the 2/1 commensurability with Jupiter, we will not average it with respect to both the mean longitudes λ of the asteroid and $\lambda_{\rm jup}$ of Jupiter, but we will retain all the terms in $\lambda - 2\lambda_{\rm jup}$. Indeed $\lambda - 2\lambda_{\rm jup}$ can be considered as a new "slow" angle of the problem.

Taking into account the d'Alembert properties, one easily sees that the Fourier expansion of the perturbation caused by Jupiter, assuming its eccentricity and inclination equal to zero, has only harmonics with argument

$$n_1\lambda + n_2\lambda_{\rm jup} + n_3 h + n_4\zeta\ , \tag{1}$$

where h is the opposite of the longitude of perihelion and ζ the opposite of the longitude of the node, using Poincaré's notations. The integers n_1, n_2, n_3, and n_4, are related by the equation

$$n_1 + n_2 = n_3 + n_4\ , \tag{2}$$

and n_4 is even. Putting now in evidence in (1) the term $\lambda - 2\lambda_{\rm jup}$, and using (2) the argument becomes

$$n_1(\lambda - 2\lambda_{\rm jup}) + (n_2 + 2n_1)\lambda_{\rm jup} - n_1 h + (n_2 + 2n_1 - n_4)h + n_4\zeta\ . \tag{3}$$

If one averages the Hamiltonian with respect to the fast angle $\lambda_{\rm jup}$, only the terms with $n_2 + 2n_1 = 0$ survive, namely one has the argument

$$n_1(\lambda - 2\lambda_{\rm jup} - h) + n_4(\zeta - h)\ . \tag{4}$$

This quick analysis guides us in the definition of suitable canonical variables. First of all we choose units of mass, length and time such that $G = 1$, $\mu + m_{\rm jup} = 1$, $d_{\odot-{\rm jup}} = 1$, where G is the gravitational constant, μ the mass of the Sun, $m_{\rm jup}$ that of Jupiter and $d_{\odot-{\rm jup}}$ the distance between Jupiter and the Sun, so that the mean motion of Jupiter turns out to be equal to 1. We start from the modified Delaunay variables

$$\begin{aligned} \Lambda &= L & \lambda &= l + g + \vartheta \\ H &= L - G & h &= -g - \vartheta = -\varpi \\ Z &= G - \Theta & \zeta &= -\vartheta\ , \end{aligned} \tag{5}$$

where $L = \sqrt{\mu a}$, $G = L\sqrt{(1-e^2)}$ and $\Theta = G\cos i$, with the usual notations a, e, i for semi-major axis, eccentricity and inclination of the asteroid; moreover g is the argument of perihelion, ϑ the longitude of node, and l the mean anomaly, as denoted by Poincaré. Furthermore, since the Hamiltonian is time-dependent through the mean longitude of Jupiter $\lambda_{\rm jup}$, we extend the phase space adding the new conjugated pair $\Lambda_{\rm jup}, \lambda_{\rm jup}$. With these settings, the unperturbed Hamiltonian of the Keplerian problem can be written as

$$-\frac{\mu}{2\Lambda^2} + \Lambda_{\rm jup}\ . \tag{6}$$

Furthermore, we introduce the new variables

$$\begin{aligned} S &= H + Z = L - \Theta & \sigma &= -\lambda + 2\lambda_{\rm jup} + h \\ Z &= Z = G - \Theta & g &= \zeta - h \\ N &= \Lambda + S = 2L - \Theta & \nu &= \lambda - 2\lambda_{\rm jup} \\ B &= 2\Lambda + \Lambda_{\rm jup} & \lambda_{\rm jup} &= \lambda_{\rm jup}\ . \end{aligned} \tag{7}$$

One easily recognizes that the angles σ and g are the only two which are present in (4). The angle g is the argument of perihelion, while σ is generally called the critical angle of the resonance.

The operation of averaging with respect to $\lambda_{\rm jup}$ is supported, from the point of view of perturbation theory, by the fact that the unperturbed part of the Hamiltonian (6) in the new variables reads

$$-\frac{\mu}{2(N-S)^2} + B - 2(N - S) \tag{8}$$

and, in the neighbourhood of the point $N_0 - S_0 = L_0$ such that $\mu/L_0^3 = 2$ (the 2/1 mean motion resonance), only the derivative with respect to B is large. The average with respect to $\lambda_{\rm jup}$ can be made using the Lie algorithm of normalization. The latter introduces new terms of higher degree in the mass of Jupiter. As these terms are small (here there are no small denominators), we will neglect them in the following.

The averaged Hamiltonian obtained corresponds to a system with three degrees of freedom. However, the action N turns out to be a constant of motion of the problem, since the conjugated angle ν is not present in (4). On a given surface $N = \sqrt{\mu a}(2 - \sqrt{1-e^2}\cos i)$ =constant, the problem can be regarded as described by a two degrees of freedom Hamiltonian, so that it can be studied applying the technique of successive elimination of harmonics as in Morbidelli (1993). To have a complete description of the phase space, however, a suitable number of these surfaces should be studied. As we are interested here in the dynamics between 2.91 and 3.28 A.U. at quite

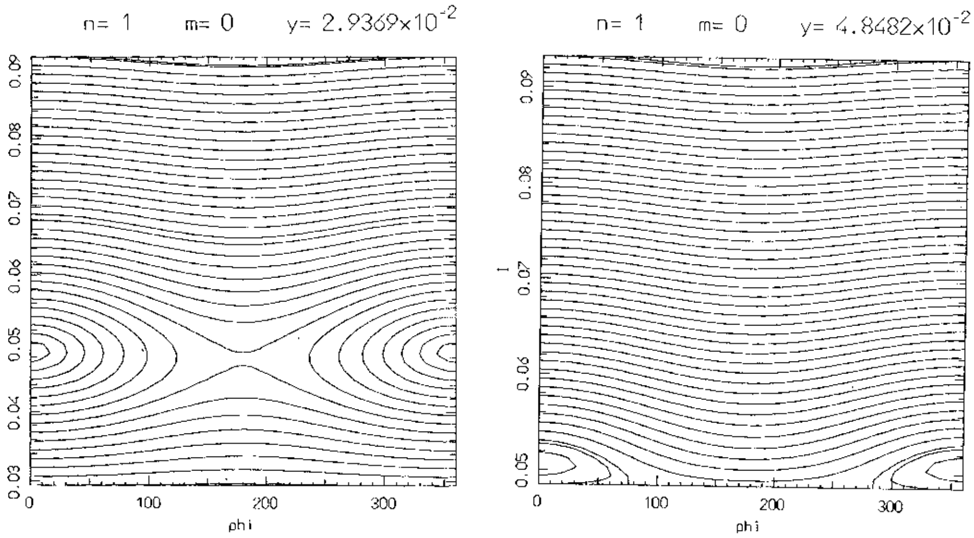

Fig. 2. a and b. Picture **a**, on the left: the phase portrait in the variables σ, S for a given value of $y \equiv Z$ ($Z = 2.9369 \times 10^{-2}$, $N = 0.841566$). Picture **b**, on the right: the same for $Z = 4.8482 \times 10^{-2}$, $N = 0.841566$

large inclinations (i.e. greater than 10 degrees), we will study in the following 5 different surfaces. For fixed values of the eccentricity, equal to 0.1, 0.15, 0.2, from left to right, these surfaces are represented in a (a, i) diagram by the dashed curves reported in Figs. 6, 7 and 8.

3. The application of the method of successive elimination of harmonics

The first step for the application of the algorithm of successive elimination of harmonics is the computation of the expansion of the Hamiltonian in Fourier series of the angles on each surface in analysis. We are interested here to study orbits with an eccentricity not exceeding 0.4 (this limit is chosen also to guarantee a fast convergence of the Fourier expansion of the Hamiltonian with respect to σ). This gives a bound in the variables S, Z on each surface. Furthermore we define a suitable grid of 200 points in the action space (S, Z) and, at each point, we compute the Fourier expansion of the Hamiltonian. This requires to average the original Hamiltonian with respect to $\lambda_{\rm jup}$ and to evaluate it for several values of the angles σ and g in order to apply the fast Fourier transform algorithm. In this way we have computed the expansion

$$\sum_{n,m} h_{n,m}(S, Z) \cos(n\sigma + 2mg) , \tag{9}$$

with $0 \leq n \leq 20$ and $-10 \leq m \leq 10$. At the same time we have computed the derivatives with respect to the actions of the main term $h_{0,0}$ (independent of the angles) in order to have a first approximation of the frequencies. On the base of this grid in the action space, we then compute the Fourier expansion of the Hamiltonian and its derivatives on any point (S, Z) using a cubic-spline interpolation as explained in Morbidelli (1993); the derivatives of the coefficients $h_{n,m}$ of the harmonics are computed as the derivatives of the interpolation function.

We point out here that three frequencies, instead of two, have to be computed in this case. Indeed, the frequencies of σ and g are needed to study the dynamics on the surface, as usual; the frequency of the longitude of perihelion $-h$ is needed to determine the location of secular resonances (the frequency of the longitude of the node is determined in turn, as one knows that of g). This causes a series of technical complications. First of all the main term $h_{0,0}$ must be derived with respect to S, Z and also with respect to N, in order to compute the frequency of h as $\partial h_{0,0}/\partial S + \partial h_{0,0}/\partial N$. Furthermore, we need also the derivative with respect to N of the coefficient of each harmonic. For this reason, for each surface N =constant we are interested in, we actually study a package of 3 surfaces very close to it.

The basic idea of the algorithm of successive elimination of harmonics is very simple. First one harmonic is isolated (for example choosing the one with the most relevant dynamical effect); since an Hamiltonian with only one harmonic in its spectrum is integrable, such an harmonic is eliminated introducing suitable Arnold action–angle variables (Arnold 1963); afterwards, the new variables are introduced in the part of the Hamiltonain which was neglected (i.e. all the other harmonics in the perturbation) and the Fourier expansion in harmonics of the new angles is computed again; finally the algorithm is iterated, by looking for the new most relevant harmonic to be eliminated.

In our case, a graphical analysis of the different terms in the expansion (9) shows that the harmonic with argument σ is the one which has the most relevant dynamical effect. Moreover, σ is also the angle characterized by having the shortest period of circulation/libration. Therefore, we first proceed in the elimination of this harmonic. The harmonic is eliminated for different constant values for the action Z (each one corresponding, approximately, to a different value of the inclination). The two typical portraits of the dynamics described by the simplified Hamiltonian, where only the harmonic in σ is retained, are those shown in Fig. 2, which refer to the same value of N and different values of Z. The Arnold angle–action variables are introduced in the region where σ circulates with negative derivative, i.e. the region with semi–major axis a smaller than the one corresponding to the 2/1 resonance. This is the upper

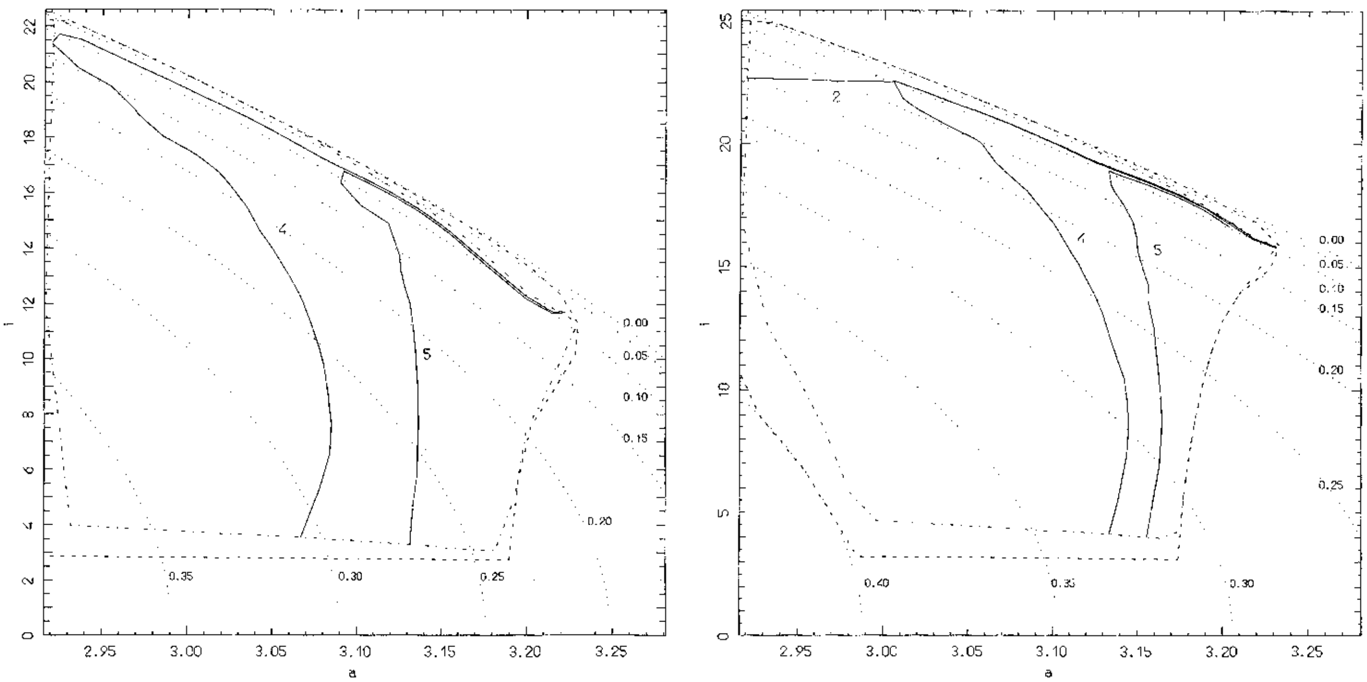

Fig. 3. a and b. Secular resonances on two surfaces related to two different values of N (N = .80576 on the left and N = .82075 on the right). The dotted lines mark the location of the surface for different values of the eccentricity, from 0 to 0.4, indicated near the corresponding line. The dashed line is the border of the region where the action–angle variables are defined for the elimination of the first harmonic, with argument σ. The dashed–dotted line is the border of the region where action–angle variables are defined to eliminate the second harmonic, with argument g. Finally the continuous lines mark the location of secular resonances. Note how the secular resonances bend approaching the line $e = 0$

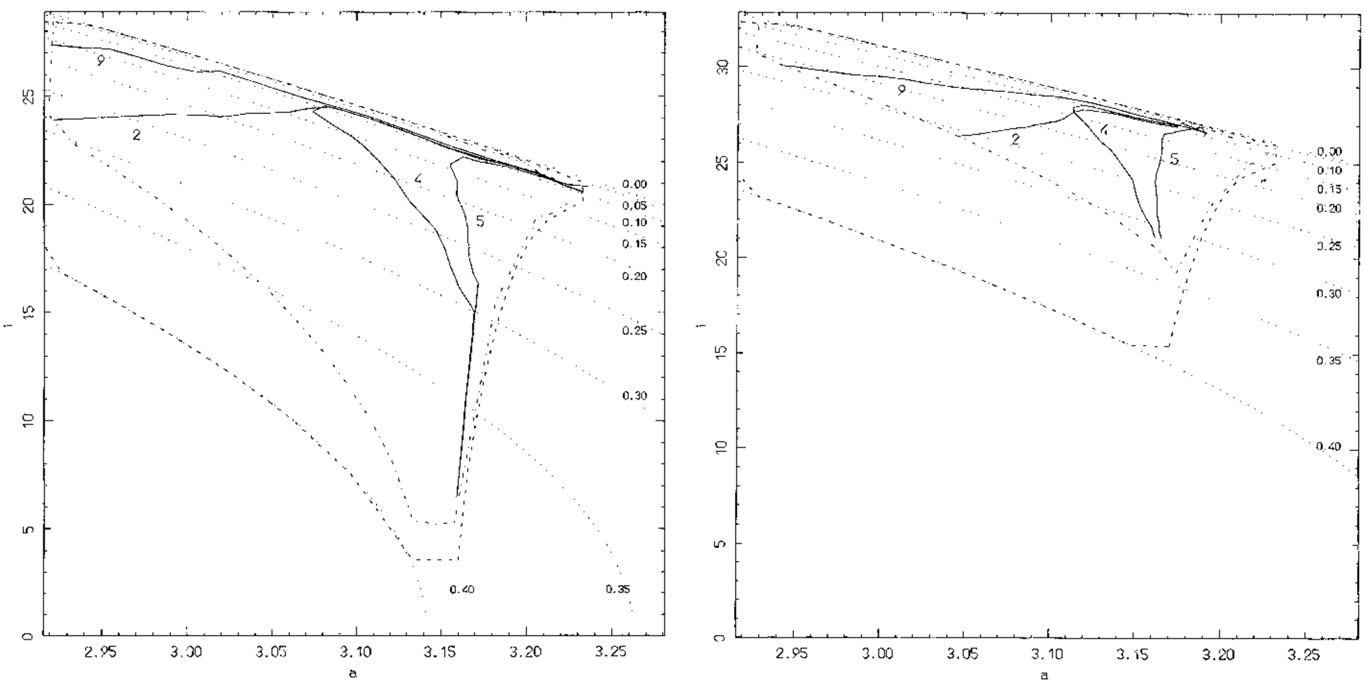

Fig. 4. a and b Secular resonances on surfaces related to two more different values of N (N = .84156 on the left and N = .868064 on the right). See text for comment

region in Fig. 2a, above the separatrix of the 2/1 resonance. On the contrary, in Fig. 2b only one equilibrium point exists, and no separatrix is present. Since the border at the bottom of Fig. 2b corresponds to $e = 0$ and σ is not defined there, an orbit that collides against the border at the right bottom corner of the picture comes out of the border at the left bottom corner. In polar coordinates this would give a picture where the center of rotation is translated with respect to the origin of the coordinates. The new action angle variables are introduced, for simplicity, only in the region above the torus which is tangent in $\sigma = 180°$ to the bottom border of Fig. 2b.

The next step of the algorithm of successive elimination of harmonics is to take into account the motion of the argument of perihelion. Indeed, the most relevant harmonic of the Hamiltonian expressed in the new action–angle variables turns out to be the one with argument $2g$, or, more precisely, $2\psi_g$, where ψ_g is the transformed of g via the previous Arnold action–angle variable transformation. We are interested here in the region of counterclockwise circulation of this angle ($\dot{g} > 0$), as in the above mentioned works on the location of secular resonances.

At this step, the size of the chaotic layers estimated by looking at the tori that collide with the separatrix of the previously eliminated harmonic, appears to be very small. Indeed, the motion of σ affects the S variable only, whereas the motion of g affects the Z variable only, so that the possibility of a collision is limited to a narrow region.

For what regards secondary resonances, these turn out to have a negligible effect, except very close to the separatrix of the σ harmonic. Therefore, after the elimination of the harmonics in σ and in $2g$, the new action variables seem to be fairly constant. For this reason we believe the proper frequencies computed at this stage to be sufficiently precise. In the next section we will then discuss the location of secular resonances.

4. The location of secular resonances close to the 2/1 commensurability

We illustrate our theoretical results in Figs. 3,4 and 5. Each picture refers to a different surface N =constant. The dotted lines denote the location of the surface N =constant on the (a, i) diagram for different values of the eccentricity, from 0 to 0.4, indicated near the corresponding line. The dashed and the dashed–dotted lines delimit the domains where we have performed the elimination of the first (σ) and the of second harmonic (g) respectively. The shape of these domains in the $a - e - i$ space depends on the values of the angles σ and g. Here we represent them on the section $\sigma = 0, g = 0$. More precisely, the dashed curve is the border of the region of circulation of σ where the new action–angle variables are first introduced. In particular the right border is the separatrix of the 2/1 mean motion resonance. Conversely, the dashed-dotted curve is the border of the region of circulation of g where new action–angle variables are introduced at the second step. As it is well known, the effect of the motion of the argument of perihelion is to increase the eccentricity, which takes a maximum at $g = 90°$. The effect is particularly significant at large inclination, so that only

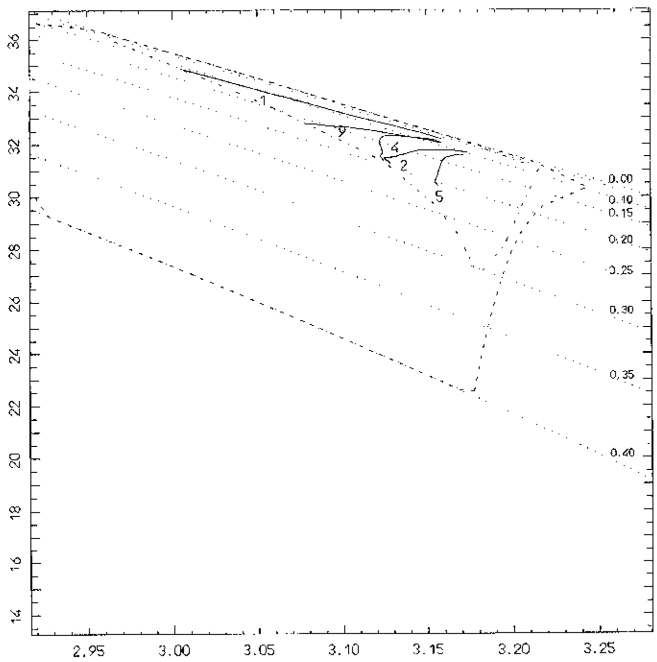

Fig. 5. Secular resonances on the surface N = .900036

the orbits with very small eccentricity at $g = 0$ do not exceed the limit value 0.4 that we have (arbitrarily) imposed. This explains why the region where the new action–angle variables are introduced becomes narrower passing from Fig. 3a to Fig. 5. Indeed, the surfaces N =constant, which these figures refer to, are ordered by increasing values of the inclination.

In the region delimited by the dashed–dotted curve, we have computed, via the elimination of the two relevant harmonics in σ and g, the proper frequencies of the system. Now, to compute the location of secular resonances, it is just a matter of comparing the proper frequencies calculated above with the proper frequencies of the Solar System. This is done simply using a level curve graphic routine. In this case, however, the proper frequencies have been computed on a non–regular grid (made up of 400 points), so that a suitable routine had to be designed.

In Figs. 3, 4 and 5 the secular resonances are indicated by continuous lines. The nomenclature is that adopted by Milani & Knežević(1990) and is the following: **1** $\nu_{h'} = g_5$; **2** $\nu_{h'} = g_6$; **4** $\nu_{h'} + \nu_{\zeta'} = g_5 + s_6$; **5** $\nu_{h'} + \nu_{\zeta'} = g_6 + s_6$; **9** $2\nu_{h'} = g_5 + g_6$. Here we have indicated by $\nu_{h'}$ and $\nu_{\zeta'}$ the proper frequencies of the longitude of perihelion and of the longitude of node called g ans s by Milani and Knežević. g_5, g_6 and s_6 are the proper frequencies of the Sun–Jupiter–Saturn system. As one sees, such lines are not perfectly smooth; this can give a quantitative idea of the indetermination of the results due to numerical errors.

In Figs. 3, 4 and 5 the pictures refer to the surfaces N =constant ordered by increasing value of the inclination. On the first one (Fig. 3a), only the resonance **4** and **5** are present. As discussed in Milani & Knežević ((1990, 1991)), the latter is the resonance that has a dominant role in the dynamics of the Eos family.

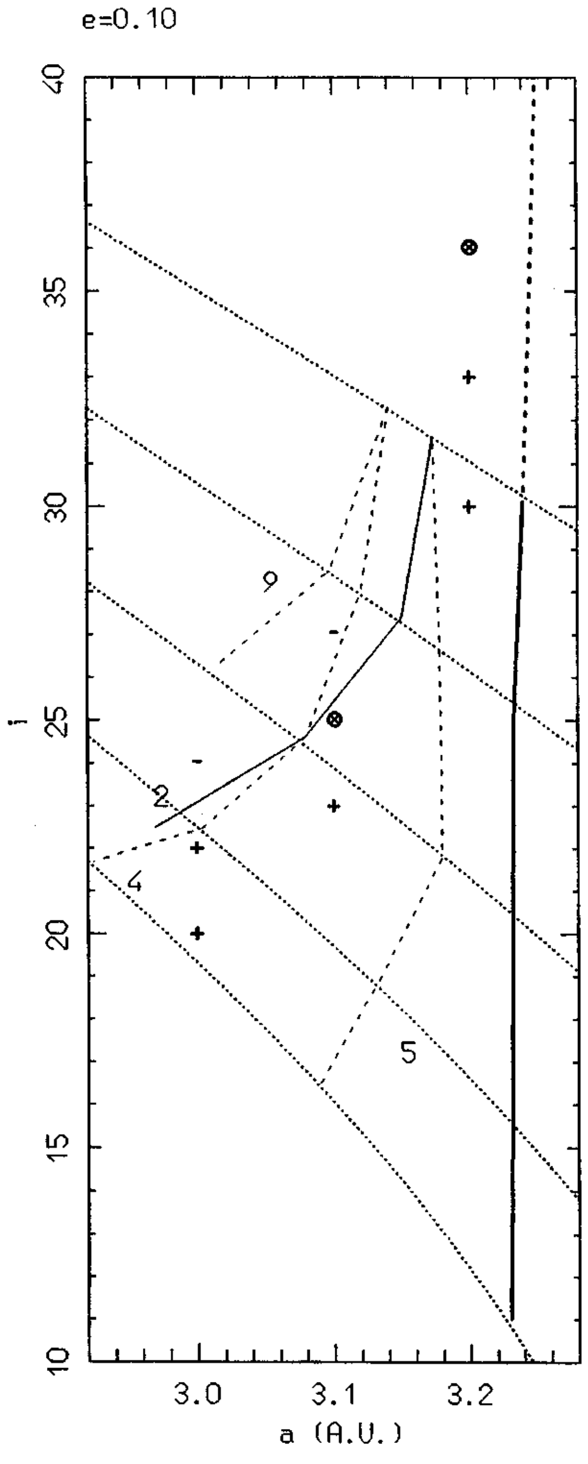

Fig. 6. The location of secular resonances in an a, i diagram computed for a proper eccentricity (value of e when $\sigma = g = 0$) equal to 0.10. On each picture we indicate the border of the 2/1 commensurability. The symbols +, $-$ and 0 denote respectively orbits which are found numerically to be below, above and in the ν_6 resonance (see tex for more details)

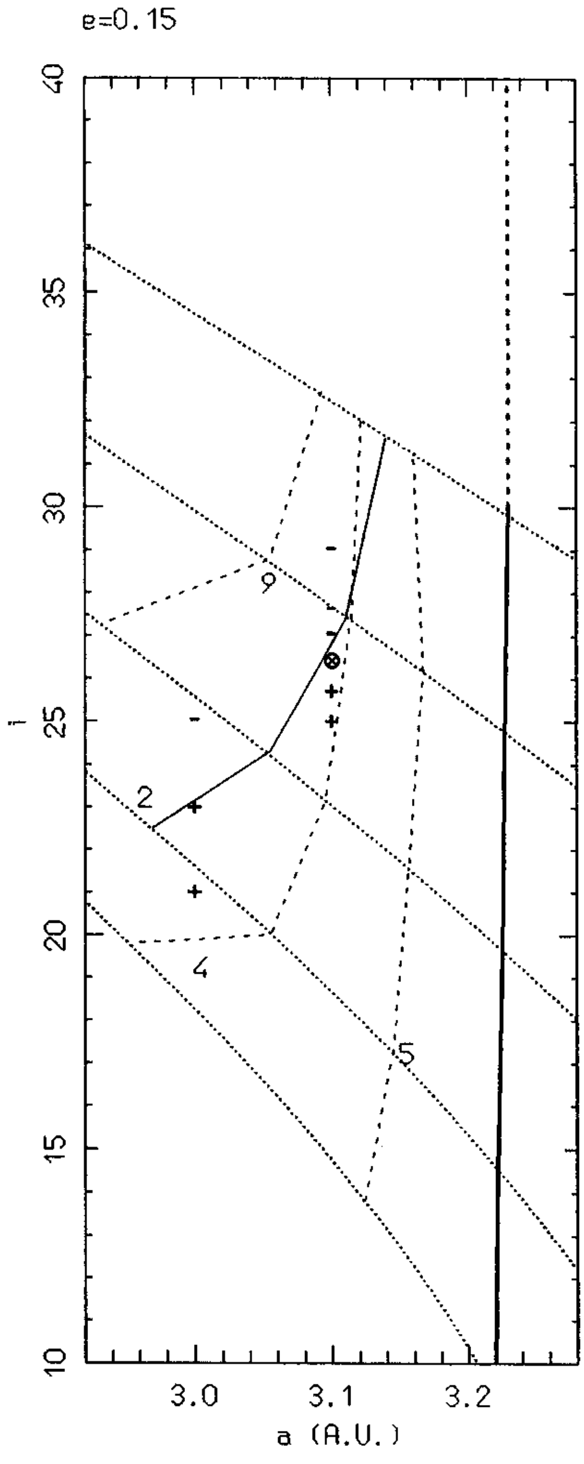

Fig. 7. The same as Fig. 6, for a proper eccentricity equal to 0.15

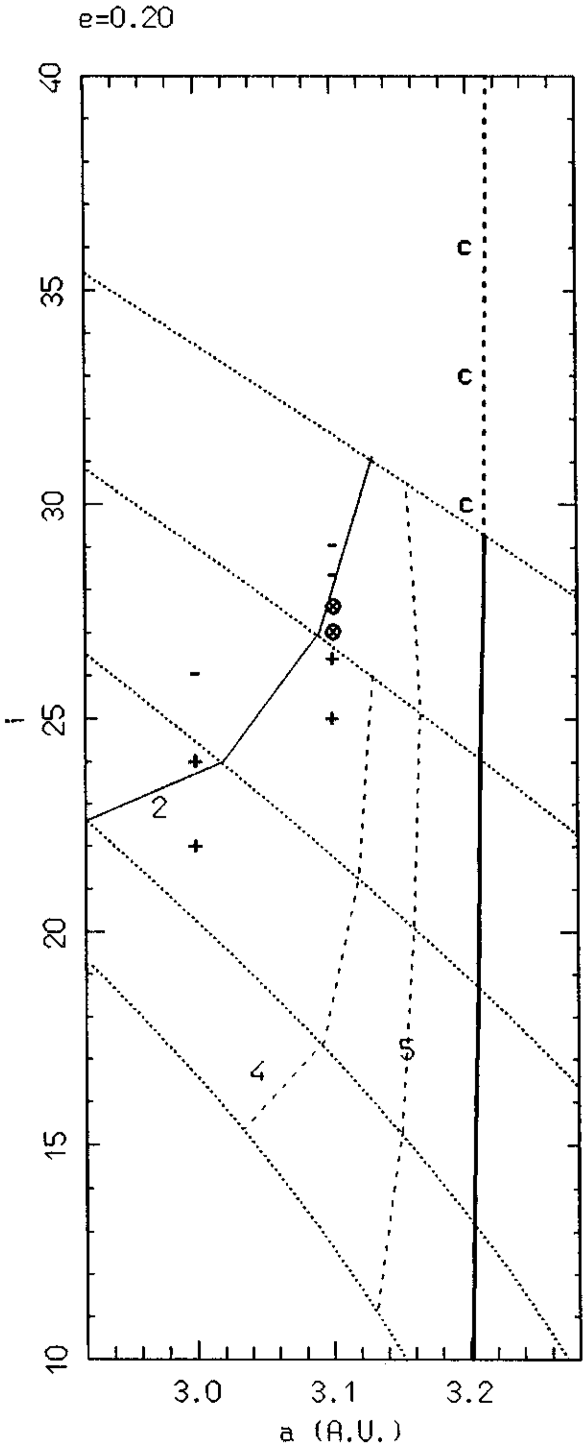

Fig. 8. The same as Fig. 6, for a proper eccentricity equal to 0.20. The *c* symbols denote orbits which are captured in the 2/1 commensurability

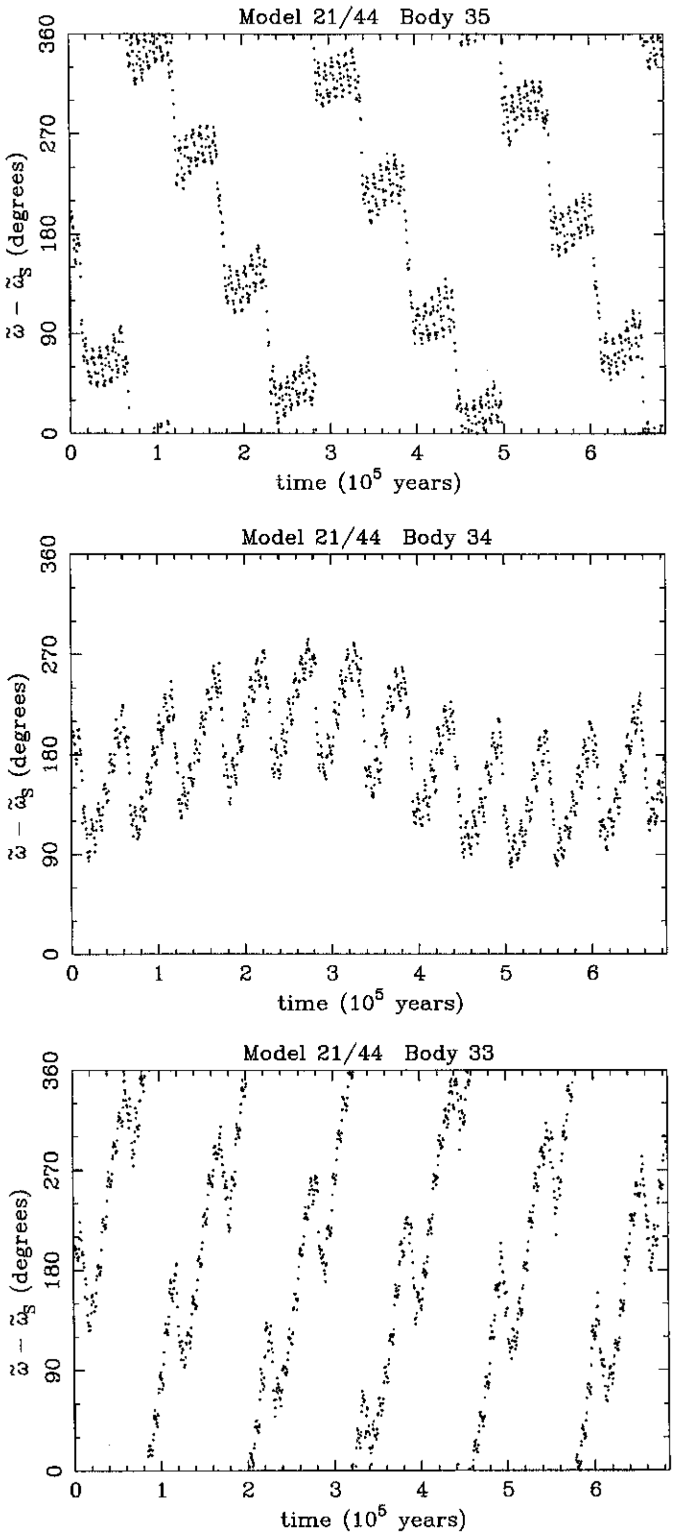

Fig. 9. a–c. Top: the critical argument of the ν_6 resonance circulates with negative derivative, denoting that the object is above the resonance. Middle: the critical argument librates around 180°, denoting that the object is in the ν_6 resonance. Bottom: the critical argument circulates with positive derivative, so that the object is below the ν_6 resonance

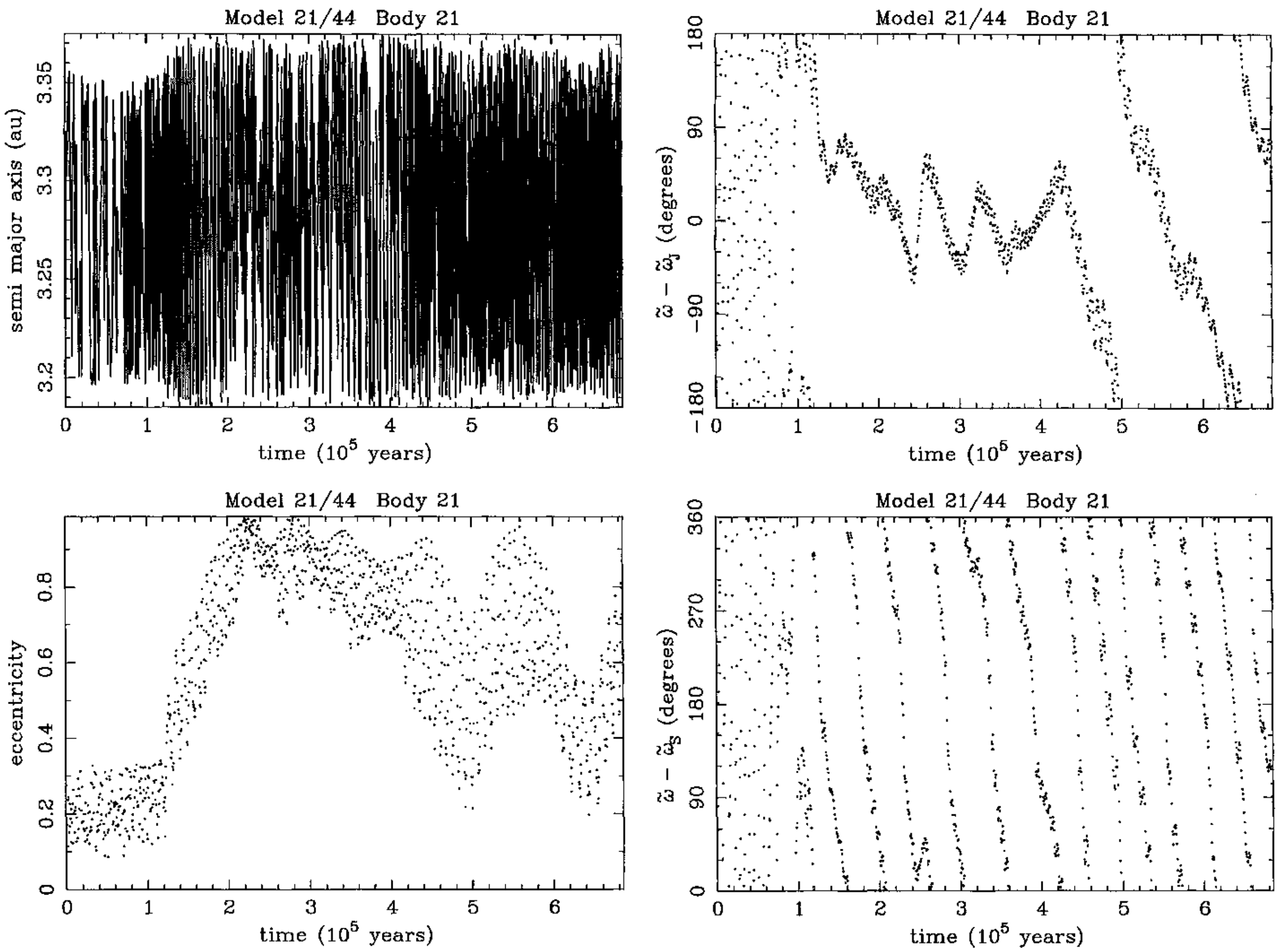

Fig. 10. a–d. Semimajor axis, eccentricity, $\varpi - \varpi_J$ and $\varpi - \varpi_S$ as functions of time for one of the orbits which are captured into the 2/1 mean motion commensurability

On the second one (Fig. 3b) also the ν_6 resonance (**2**) appears in the upper left corner.

On the third one (Fig. 4a) the resonance **9** appears.

The ν_5 resonance (**1**) appears only on the last surface, reported in Fig. 5.

The deviation which all resonances show when approaching the line of zero eccentricity is due to the fact that the frequency of the longitude of perihelion becomes negative, so that all values corresponding to commensurabilities are crossed. As a consequence, all secular resonances appear to cluster together at small eccentricities. This could give rise to a very complicated dynamics, but we think that the effect of secular resonances should not be very strong in this region, since the proper frequency of perihelion changes very fast with the eccentricity. We must point out, however, that in this region our results could be poor from the quantitative point of view, since one is working close to a singularity of the original action–angle variables.

In order to have a direct comparison with the usual pictures on the location of secular resonances reported in Williams & Faulkner (1981), Milani & Knežević(1990, 1991) and Morbidelli & Henrard (1991), we have plotted in Figures 6, 7 and 8 the location of secondary secular resonances (dashed lines) in 3 different (a, i) diagrams, related to fixed values of the proper eccentricity equal to 0.10, 0.15, and 0.20 respectively. The location of the ν_6 resonance is plotted by a solid line. We recall that these diagrams are computed for $\sigma = g = 0$. The bold line on the right side of each picture is the location of the left border of the 2/1 resonance. As one sees, it bents slowly to the right since the width of the 2/1 resonance becomes narrower with increasing values of the inclination. Moreover, as already anticipated at the end of section 2, the dotted lines denote the position of the surfaces N =constant on which the computations have been performed.

From a qualitative point of view, Figures 6, 7 and 8 confirms the conjecture that the secular resonances are deviated at larger inclinations when approaching the 2/1 mean motion resonance.

In order to confirm our result from the quantitative point of view, we have performed many numerical integrations choosing the initial conditions in a systematic way on a suitable grid. All initial conditions are chosen with $\sigma = 0$ and $g = 0$, in order to be consistent with Figs. 3, 4, 5 and 6, 7, 8. We have tested three values of the semi major axis, i.e. 3.0, 3.1 and 3.2 A.U. Initial eccentricities are 0.10, 0.15 and 0.20 as in Figs. 6, 7 and 8. Finally, we choose several values of the inclination, with a stepsize of 2 degrees. Moreover, for each of these sets $a, e, i, \sigma = 0, g = 0$ we have integrated two orbits, one with initial $\varpi - \varpi_S = 0$, the other with $\varpi - \varpi_S = 180°$, where ϖ is the longitude of perihelion of the asteroid, ϖ_S that of Saturn and $\varpi - \varpi_S$ is the critical angle of the ν_6 resonance.

We stress the importance of the choice of our initial conditions at $\sigma = 0$ and $g = 0$; the conversion from the proper action variables to the osculating a, e, i has been made in all the figures of this paper at $\sigma = 0, g = 0$. Therefore, the values of a, e, i in correspondence with these values of the angles, can be considered as a sort of *proper elements* for our theory. It is true, however, that our theory on the location of secular resonances does not take into account the part of the Hamiltonian which depends on the critical angles of secular resonances, but only the approximation obtained assuming the planets on coplanar circular orbits, called $\overline{K_0}$; in other words, in our theory resonances are surfaces in the space of proper frequencies, while in the real system (the one we integrate numerically) resonances have a given width, with libration regions and possibly chaotic zones. Our choice of integrating two orbits, one with initial $\varpi - \varpi_S = 0$, the other with $\varpi - \varpi_S = 180°$, takes this fact into account. As a matter of fact, these two orbits are different in the ideal proper element space (a space which no one is able to compute in this region up to now), while they are the same in approximate proper element space given by our theory. Therefore, our numerical integrations will provide an estimate of the real width of the ν_6 resonance and of the accuracy of our results with respect to the real system.

In Figs. 6, 7, and 8 we show our numerical findings in a synthetic way. The + symbols mark the initial conditions of those fictitious asteroids which turn out to lie *below* the ν_6 resonance (i.e. $\varpi - \varpi_S$ circulates with positive derivative). The − symbols mark the initial conditions of those bodies which are *above* the ν_6 resonance (i.e. $\varpi - \varpi_S$ circulates with negative derivative); finally the 0 symbols indicate orbits which are found *in* the ν_6 resonance (i.e. $\varpi - \varpi_S$ librates). An example is given in Fig. 9, which refers to three orbits which have all the same initial semimajor axis a = 3.1 A.U., eccentricity e = 0.10 and different inclinations equal to 23, 25 and 27 degrees respectively from bottom to top. Librations are found only around $\varpi - \varpi_S = 180°$.

In order to have a better experimental estimate on the location of the ν_6 resonance at a = 3.1 A.U., we have performed a sequence of 8 additional numerical integrations on a grid with a smaller stepsize in inclination. These orbits are also marked Figs. 6, 7, 8 with the same symbols explained above.

As one sees, the results are somewhat poor for a = 3.0 A.U., probably due to the nearby presence of the weak 7/3 mean motion commensurability. The numerical integrations confirm on the contrary with good accuracy our theoretical findings at a = 3.1 A.U. Somewhat different is the result at a = 3.2 A.U.. Indeed all orbits with initial eccentricity e = 0.20, denoted in Fig. 8 with a c symbol, are captured into the 2/1 commensurability, therefore confirming our theoretical computations on the location of the border of the 2/1 commensurability. These captured orbits exhibit a very complicated dynamics as shown in Fig. 10 for one of them (initial i = 30°, and $\varpi - \varpi_S = 0°$); the semimajor axis oscillates around 3.28 A.U., denoting capture in the 2/1 commensurability; the eccentricity grows to very large values (0.95). The mechanism responsible for this large growth of the eccentricity seems to be the ν_5 resonance; indeed its critical angle $\varpi - \varpi_J$ varies very slowly, while the ν_6 resonance looses importance since its critical argument $\varpi - \varpi_S$ circulates rapidly. This fact is not surprising; indeed, as shown in Morbidelli & Moons (1993), *inside* mean motion commensurabilities the location and the strength of secular resonances is completely different and the ν_5 resonance is the dominating one.

At a = 3.2 A.U. only orbits with initial eccentricity e = 0.1 avoid the 2/1 commensurability; among these orbits, only the one with initial i = 36°is in the ν_6 resonance. This orbit has a very strange behaviour, alternating between circulation and libration of the critical angle $\varpi - \varpi_S$.

References

Arnold, V. I. 1963. On a theorem of Liouville concerning integrable problems of dynamics , *Sib. mathem. zh.*, **4**, 2.

Kozai, Y. 1962. Secular perturbations of asteroids with high inclination and eccentricities. *Astron. J.*, **67**, 591–598.

Lemaitre, A., and Morbidelli, A. 1992. Computation of proper elements for high inclined asteroids. Submitted to *Celest. Mech.*

Milani, A., and Knežević, Z. 1990. Secular perturbation theory and computation of asteroid proper elements. *Celest. Mech.*, **49**, 247–411.

Milani, A., and Knežević, Z. 1992. Asteroid proper elements and secular resonances. *Icarus*, **98**, 211–232.

Morbidelli, A., and Henrard, J. 1991. Secular resonances in the asteroid belt: theoretical perturbation approach and the problem of their location. *Celest. Mech.*, **51**, 131–167.

Morbidelli, A.1993. On the successive eliminations of perturbation harmonics. *Celest. Mech.*, **55**, 101–130.

Morbidelli, A., and Giorgilli, A. 1993. A quantitative perturbation theory by sucessive elimination of harmonics. *Celest. Mech.*, **55**, 131–159.

Morbidelli, A., and Moons, M. 1993. Secular resonances inside mean motion commensurabilities: the 2/1 and 3/2 cases. *Icarus*, in press.

Williams, J. G. 1969. Secular perturbations in the solar system. *Ph.D. dissertation*, University of California, Los Angeles.

Williams, J. G., and Faulkner, J. 1981. The position of secular resonance surfaces. *Icarus*, **46**, 390–399.

This article was processed by the author using Springer-Verlag LaTeX A&A style file version 3.